Shock Fluctuations in the Two-Dimensional Asymmetric Simple Exclusion Process*

Francis J. Alexander,[†] Zheming Cheng,[‡]
Steven A. Janowsky[§] and Joel L. Lebowitz

Departments of Mathematics and Physics
Rutgers University
New Brunswick, NJ 08903

February 26, 1992

Abstract

We study via computer simulations (using various serial and parallel updating techniques) the time evolution of shocks, particularly the shock width $\sigma(t)$, in several versions of the two-dimensional asymmetric simple exclusion process (ASEP). The basic dynamics of this process consists of particles jumping independently to empty neighboring lattice sites with rates $p_{\text{up}} = p_{\text{down}} = p_{\perp}$, $p_{\text{left}} < p_{\text{right}}$. If the system is initially divided into two regions with densities $\rho_{\text{left}} < \rho_{\text{right}}$, the boundary between the two regions corresponds to a shock front. Macroscopically the shock remains sharp and moves with a constant velocity $v_{\text{shock}} = (p_{\text{right}} - p_{\text{left}})(1 - \rho_{\text{left}} - \rho_{\text{right}})$. We find that microscopic fluctuations cause σ to grow as t^{β}, $\beta \approx 1/4$. This is consistent with theoretical expectations.

We also study the nonequilibrium stationary states of the ASEP on a periodic lattice, where we break translation invariance by reducing the jump rates across the bonds between two neighboring columns of the system by a factor r. We find that for fixed overall density ρ_{avg} and reduction factor r sufficiently small (depending on ρ_{avg} and the jump rates) the system segregates into two regions with densities ρ_1 and $\rho_2 = 1 - \rho_1$, where these densities do not depend on the overall density ρ_{avg}. The boundary between the two regions is again macroscopically sharp. We examine the shock width and the variance in the shock position in the stationary state, paying particular attention to the scaling of these quantities with system size. This scaling behavior shows many of the same features as the time-dependent scaling discussed above, providing an alternate determination of the result $\beta \approx 1/4$.

KEY WORDS: Stochastic particle systems; shock waves; surface growth

*Supported in part by National Science Foundation grant DMR 89-18903.

[†]Supported in part by a Rutgers University Excellence Fellowship. Current address: Center for Nonlinear Studies, MS-B258, Los Alamos National Lab, Los Alamos, NM 87545

[‡]Current address: Program Development Corp., 300 Hamilton Ave., Suite 409, White Plains, NY 10601

[§]Supported in part by National Science Foundation Mathematical Sciences Postdoctoral Research Fellowship DMS 90-07206

1 Introduction

Macroscopic equations that describe fluid flow result from an averaging over the rapidly fluctuating microscopic motion of a large number of molecules [1]. This procedure yields deterministic (typically nonlinear) partial differential equations for the conserved quantities (momentum, energy, mass density)—which vary slowly on the microscopic scale. The familiar hydrodynamic equations of motion (Navier-Stokes and Euler) which describe the dynamics of fluids are of this form.

These equations describe quite well what happens to fluids on a large scale when the flow is smooth. Problems arise when gradients in the hydrodynamic variables become very large and the assumptions made in the derivation of the hydrodynamic equations break down—for example, where discontinuities (shocks) in macroscopic variables (such as the density) appear. We would like to gain a better understanding of these situations both at the macroscopic and microscopic levels.

1.1 The Burgers Equation

One of the simplest examples of a nonlinear macroscopic equation with a single conserved quantity is the Burgers equation,

$$\frac{\partial \mathbf{u}}{\partial t} = -\mathbf{u} \cdot \nabla \mathbf{u} + \nu \Delta \mathbf{u}, \tag{1}$$

originally proposed to study turbulence with $\mathbf{u}$ representing a velocity field [2, 3]; in our considerations, $\mathbf{u}$ will represent a scalar density field. What makes the Burgers equation interesting is that initially smooth density profiles can evolve after a finite time into traveling wave fronts. The transitions between low and high density regions in these fronts occur in very narrow spatial regions—regions with width proportional to $\sqrt{\nu}$. In the limit $\nu \to 0$ the profile becomes discontinuous and we say that shocks form. If ν is finite but small (*i.e.* microscopic) we may still refer to the narrow transition region as a shock. These shocks as given by the Burgers equation move with a deterministic velocity. We are interested in what happens to shocks when viewed on the microscopic level.

The non-viscous Burgers equation, with $\nu = 0$, can be derived rigorously from a number of computationally efficient particle models [1, 4]. The field $\mathbf{u}$ represents the space and time rescaled particle configurations, *i.e.* the hydrodynamic limit with Euler scaling in which time and space are scaled by a fixed ratio. (Certain special cases with other scalings can result in limits with $\nu > 0$.) Here we use the asymmetric simple exclusion process. On a lattice, particles hop to unoccupied neighboring sites with a drift (asymmetry) along one of the lattice directions. The hard-core exclusion (only one particle per site) is the source of the nonlinearity and provides for some interesting phenomena. Even on the microscopic scale shocks form. At this level, instead of traveling with some definite deterministic velocity, there is a a fluctuating velocity, due to the initial conditions and the dynamics, that must be superposed upon the macroscopic one. Therefore, the location of the shock will deviate from the location given by the Burgers equation by some fluctuating quantity [5].

1.2 The ASEP

The ASEP is a continuous time stochastic process in which particles occupy sites of the lattice $\mathbf{Z}^d$ and move according to simple rules. Configurations in this process are denoted by $\eta \in \{0,1\}^{\mathbf{Z}^d}$, where the individual site occupation variable $\eta(\vec{\mathbf{r}}) = 1$ if $\vec{\mathbf{r}}$ is occupied, and 0 if unoccupied. An exclusion rule prevents more than one particle from simultaneously inhabiting the same site. Independently and randomly, each particle waits for an exponentially distributed time with mean 1 and attempts to jump to a neighboring site. If the target site is unoccupied, then the jump succeeds; if not, then it fails. An asymmetry enhances jump attempts in one direction and induces a net particle current. In the one-dimensional model, a particle attempts to jump to the right with rate p_{right} and to the left with rate p_{left}, $p_{\text{right}} > p_{\text{left}}$, $p_{\text{right}} + p_{\text{left}} = 1$. In higher dimensions the asymmetry along the x axis persists, but the jump rates along both directions of the perpendicular axes are equal (symmetric) and given by $p_\perp$ such that $p_{\text{left}} + p_{\text{right}} + 2(d-1)p_\perp = 1$, recalling that d is the dimension. Shocks will now correspond to $(d-1)$-dimensional fronts which will fluctuate in space and time.

1.3 Shock Growth = Surface Growth; KPZ approach

We may also interpret the shock evolution in the d-dimensional ASEP as a model of $(d-1)$-dimensional surface growth where holes are driven to the left and stick to the "hole substrate," with the surface of this substrate traveling to the right. This interpretation is particularly useful given the recent interest in surface deposition models and the kinetic roughening of surfaces [6]. The model we describe here is complicated for analysis as well as for simulation since we are interested in the statistics of the shock (= surface) and its dependence on a priori *unknown* properties of the ASEP. In other surface problems one usually assumes that the particles (or holes) hitting the surface are uncorrelated or have *known* correlations. One can then construct a stochastic partial differential equation which models the surface dynamics.

Typically the approach to such problems in surface roughening models is to introduce a Langevin type equation which governs the local interface position $h(\vec{\mathbf{r}}, t)$, the usual choice being the Kardar-Parisi-Zhang (KPZ) equation [7]:

$$\frac{\partial h}{\partial t} = v_0 + \nu \Delta h + \frac{\lambda}{2}(\nabla h)^2 + \zeta(\vec{\mathbf{r}}, t). \tag{2}$$

The random noise term $\zeta(\vec{\mathbf{r}}, t)$ is such that

$$\langle \zeta(\vec{\mathbf{r}}, t) \rangle = 0, \tag{3}$$

but otherwise is chosen according to the specific nature of the model being studied [8].

The KPZ equation provides a phenomenologically based description of a growing surface. Each term represents a different aspect of the growth process: the constant v_0 is the growth rate for a completely flat interface. The Laplacian term accounts for surface restructuring as particles diffuse on the surface and move to fill gaps, while the nonlinear gradient term describes an inclination dependent growth rate. The noise term represents growth due to fluctuations at the microscopic level; without this term the KPZ equation (2) can be related to the Burgers equation (1) via the transformation $\mathbf{u} = -\nabla h$. Higher order terms are not included in the KPZ equation because they are irrelevant in the renormalization group sense; without loss of generality we change variables $h \to h - v_0 t$ and take $v_0 = 0$.

1.3.1 Linearized KPZ

We believe that the one-dimensional KPZ equation, with the nonlinear term absent ($\lambda = 0$), describes the interface behavior of the two-dimensional ASEP. (This reduces to a noisy, linear diffusion equation.) We argue this on several grounds. In the first place, the nonlinear term arises from the dependence of surface growth on the local orientation. In the ASEP, however, the shock velocity is independent of surface orientation and so averaging over orientations results in cancellation of the nonlinear term [4].

Secondly, in the case of weak asymmetry, where $p_\perp$ is fixed, $p_{\text{right}} - p_{\text{left}} = \epsilon$, space is rescaled by ϵ and time is rescaled by ϵ^2, it is known rigorously that the equation describing the interface fluctuations in the limit $\epsilon \to 0$ is indeed just the linear KPZ equation [9]

$$\frac{\partial h(r,t)}{\partial t} = \nu \Delta h(r,t) + \zeta(r,t), \tag{4}$$

with $\zeta(r,t)$ Gaussian white noise: $\langle \zeta(r,t) \rangle = 0$ and

$$\langle \zeta(r,t)\zeta(r',t') \rangle = K\delta(r-r')\delta(t-t'), \tag{5}$$

where K depends on the asymptotic densities on either side of the interface. One can solve (4) exactly by using Fourier transforms; the result for the shock width starting with an initially flat interface in a strip of width W is [10]

$$\sigma(t) \sim \begin{cases} t^\beta, & t \ll W^{\alpha/\beta}, \\ W^\alpha, & t \gg W^{\alpha/\beta}; \end{cases} \tag{6}$$

where

$$\sigma^2(t) \equiv \frac{1}{W} \int dr\ \left(h(r,t) - \bar{h}(t)\right)^2, \qquad \bar{h}(t) \equiv \frac{1}{W} \int dr\, h(r,t), \tag{7}$$

W is the width of the system (length of the interface) and the scaling exponents are

$$\alpha = 1/2, \qquad \beta = 1/4. \tag{8}$$

We shall see later that these exponents are indeed consistent with the results of our simulations—although the approach to scaling behavior can take a very long time.

1.3.2 Logarithmic Correction

In fact there is a defect in the above analysis; the two-dimensional ASEP is known to exhibit superdiffusive behavior [11] and thus one should not expect a linear diffusion equation to accurately model it. Analysis similar to that of [12] indicates that the correct behavior is [13]

$$\sigma(t) \sim t^{1/4}(\log t)^{1/3} \quad \text{for} \quad t^{1/4}(\log t)^{1/3} \ll W^{1/2}, \tag{9}$$

while for $t^{1/4}(\log t)^{1/3} \gg W^{1/2}$ the result remains $W^{1/2}$. This correction is sufficiently small that it will be unobservable in any numerical simulation likely to be done before the next century, and (4) remains a reasonable approximation.

2 Models

We studied two basic classes of systems undergoing ASEP dynamics: The time-dependent behavior of an effectively infinite system, and the stationary states of a finite periodic model.

2.1 Two-Dimensional ASEP—Time-Dependent Model

The specific system we considered for our time dependent studies consisted of a $W \times L$ lattice with periodic boundary conditions in the vertical (perpendicular to the field) direction. Parallel to the field no effort was made to apply suitable boundary conditions as simulations were always ended prior to the arrival of information about the boundaries. In most cases we chose the jumps to be totally asymmetric in the parallel direction, *i.e.* we took $p_{\text{left}} = 0$.

Simulation of a Continuous Time Process

Since each lattice site has an independent exponentially distributed waiting time for attempting a jump, the probability of two sites attempting to jump at the same time is zero. Thus we can simulate the ASEP dynamics in discrete time by choosing at each time step one site where we attempt to schedule a jump. All sites in $[1, W] \times [1, L-1]$ are chosen with equal probability. If the chosen site is occupied, we pick a direction $\in \{\text{up, down, right, left}\}$ with probabilities $p_\perp$, $p_\perp$, p_{right} and p_{left}, respectively. If the nearest neighbor site in the chosen direction is unoccupied, the particle jumps to that site; if it is occupied, the particle does not move for the given time step.

2.2 Stationary Model

Here we consider ASEP dynamics on an $W \times L$ torus. We break the translation invariance of this periodic system by inserting a blockage into the system between columns L and 1, which reduces the probability of a particle traveling between those two columns—a set of "slow bonds" which act as a traffic jam for the particles. In the language of driven diffusive systems, the introduction of "slow bonds" is similar to altering the driving field at this one column [14]. This blockage is analogous to a restriction in a pipe through which fluid flows; the corresponding model also provides an example of the dramatic global effects caused by a local perturbation in conservative systems which do not satisfy detailed balance [15]. It also provides an alternate method for observing the same behavior as in the time-dependent model. The one dimensional version of this system was examined in [16].

More specifically, we reduce the jump rates between columns L and 1 by a factor r, $0 \leq r \leq 1$. For $r = 1$ the model is translation invariant. For $r = 0$ the model is fully blocked; the stationary state has density one behind the blockage and density zero in front of it; there is no current flowing through the system. For $0 < r < 1$ the model has nontrivial behavior, with the stationary state satisfying the requirement that the current through any column of bonds must be independent of the column location.

In this model with a blockage we are not particularly interested in the time evolution of the shock but instead study the properties of the shock in the stationary state, and how those properties depend on system size.

2.2.1 Simulation of ASEP dynamics with blockage

The simulation of the ASEP dynamics in the periodic system with a blockage is basically the same as that in the ordinary model. All sites in $[1, W] \times [1, L]$ are chosen with equal probability. If the chosen site is occupied, we pick a direction $\in$ {up, down, right, left} with probabilities $p_\perp$, $p_\perp$, $p_{\rm right}$ and $p_{\rm left}$, respectively. We now must distinguish between the blockage and non-blockage columns. If the chosen site is in column 1 or L and the chosen direction is left or right, respectively, then the particle is attempting to jump the blockage and the attempt is completed (assuming the destination site is vacant) with probability r. Other jumps take place in the same fashion as above but are completed (assuming the destination site is vacant) with probability 1.

Of course we must allow an adequate time for this system to evolve so that we can be confident that the properties we observe are indicative of the stationary state. The necessary time is determined simply by observing the time evolution of shock width, position, etc., and waiting until they reach asymptotic values. For all system sizes except for the very largest a substantial "safety" factor was also included.

2.2.2 Parallel and semi-parallel models

In order to examine very large system sizes, we devised various modifications of the ASEP that would permit effective utilization of vector and massively parallel supercomputers. Unfortunately attempting to perform updates on all sites at once is impossible as this leads to two or more particles vying for the same site. Sublattice updating is a traditional technique; however, it may introduce spurious correlations into the model. We did have limited success with the following variations on sublattice updating:

- We were able to consider 32 different realizations of the same size system at once by treating each bit of a 32 bit word as an individual system. Although the choices for which sites to update were the same for all the systems, the choice of directions in each system were independent. We were thus able to improve the statistics over that which would have otherwise been available; the 32 (correlated) systems appeared to provide data equivalent to that which would have been given by approximately 10 truly independent systems. Most of our data sampling (for both time-dependent and stationary models) made use of this procedure.

- We considered a partial sublattice updating where 32 sites in each column (spaced $W/32$ apart) were updated simultaneously. *Qualitatively* the model remained the same, but significant correlations were introduced at vertical distances of $W/32$, $W/16$, etc. None of our quantitative data makes use of this procedure.

- In an attempt to reduce the correlations introduced by a fixed sublattice updating, we decided to examine the possibility of using a sublattice which at each step had a random origin and spacing. First fix the system width W as $W = aw_1w_2w_3w_4$, where all the factors $\{w_i\}$ are relatively prime. Thus we have four possible sublattice spacings available. Updating proceeds by first choosing a sublattice spacing (stride) w_i with probability $w_i/\sum w_i$, then choosing a site, and finally updating that site and all (vertical) translates of that site by multiples of w_i. For $W = 9 \times 10 \times 11 \times 13 = 12870$ ($a = 1$) this allowed us to update between 990 and 1430 sites simultaneously using vectorized instructions on a Cray YMP. This large speedup allowed us to examine systems that were much larger than we could have otherwise considered.

3 Time-Dependent Results

3.1 Shock identity

When studying systems with shocks, we can either wait for shocks to develop from smooth initial data, or else we can impose them on the initial data by hand. We opted for the latter approach to facilitate computer simulation. In either case we must be able to identify the location of the shock. We begin by giving a particular operational definition of what is meant by a shock at the microscopic level in one dimension.

Consider the integer lattice $\mathbf{Z}$. On each site $x \geq L/2$ we independently place a particle with probability ρ_0. All sites $x < L/2$ are empty. Asymmetry in the jump rates will drive particles to the right. At time $t = 0$ we label the leftmost particle in the system the "first" particle. As the system evolves, there is no reordering of particles since jumps are to nearest neighbor sites only (no crossing). Therefore, this "first particle" label is permanently attached to the same particle. If we view the process from the first particle, then to the left the density is always zero while to the right, the density of particles approaches ρ_0 at an exponentially (in space) fast rate, where the decay length is $1/\log(p_{\text{right}}/p_{\text{left}})$ [17]. Therefore, we have an abrupt change in particle density (over a few sites)—a shock. Accordingly, we define the shock to be located at the site containing the first particle [18], and we know that even on the microscopic scale the shock remains sharp. Note that this picture breaks down when $p_{\text{right}} = p_{\text{left}}$; in this case the behavior is purely diffusive and the average distance between the first and second particles grows like $t^{1/2}$.

In two dimensions this picture needs modification. The asymmetry drives particles to the right while allowing for diffusion in the vertical direction. What results is a right-moving, rough interface across which there is an abrupt change in average particle density. We also refer to this fluctuating interface as a shock. Now, however, the first particle in each row is no

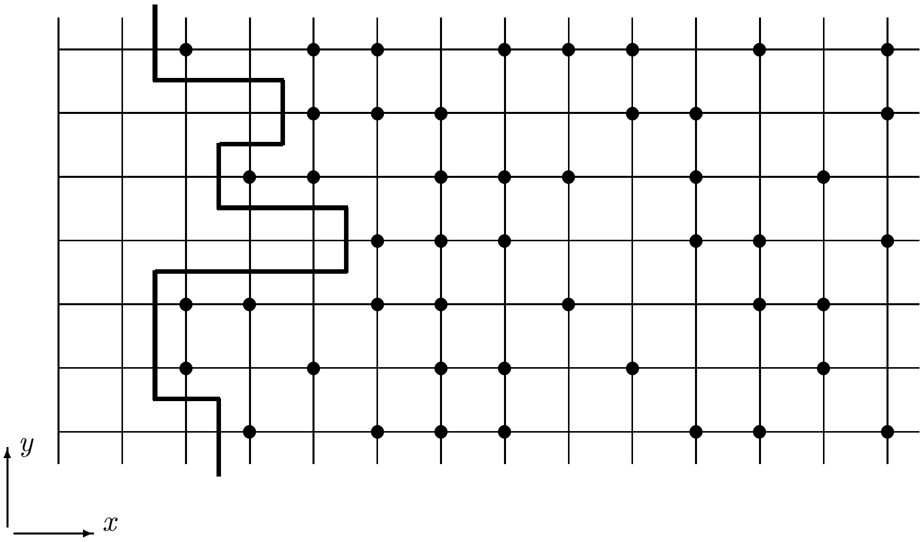

Figure 1: Example of a particle configuration and the resulting shock position $h(y,t)$.

longer a permanent label as a result of perpendicular diffusion. But the basic principle is still valid, and the most natural and computationally efficient way to characterize the shock (when the density is zero to the left) is to look at the distribution of first particles in different rows (different y values)—see Figure 1. The instantaneous width is then defined by fluctuations in these locations $h(y,t)$ about their average:

$$\sigma(t) \equiv \left(\frac{1}{W} \sum_{y=1}^{W} (h(y,t) - \bar{h}(t))^2 \right)^{1/2}, \tag{10}$$

where $\bar{h}(t)$ is the average location of the first particles,

$$\bar{h}(t) = \frac{1}{W} \sum_{y=1}^{W} h(y,t). \tag{11}$$

3.2 Results

With the exception of some limited runs to check the gross behavior with varied parameters, all of our time-dependent simulations were carried out with an initial particle density of $\rho_0 = .5$ and with jump rates $p_{\text{right}} = .75$, $p_{\text{left}} = 0$ and $p_\perp = .125$. The field drove particles to the right and holes to the left. Since particles eventually moved away from the left wall (and were not replenished) and holes moved away from the right wall (and were not replenished), we were left with particle substrate on the right of the system moving to the left, and the hole substrate on the left, moving to the right. Particle-hole symmetry (at $\rho_0 = .5$) implies they should have the same behavior. With this approach we were able to study the statistics of two nearly independent shocks at once.

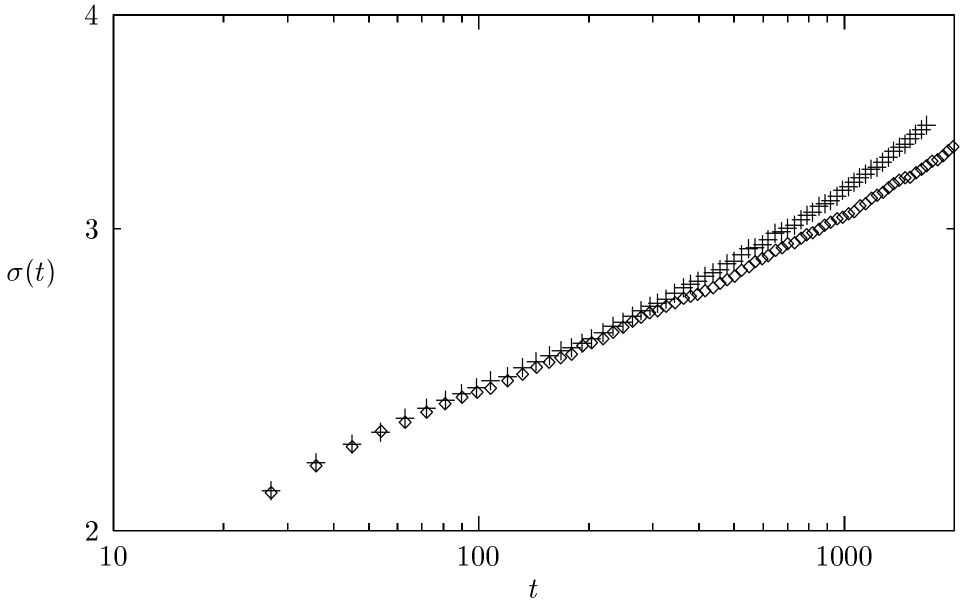

Figure 2: Shock width *vs.* time for $W = 256(\diamond)$ and $W = 1024(+)$.

In Figure 2 we compare the width of the shock interface for system widths $W = 256$ and $W = 1024$; in each case the data is averaged over 75 independent runs. The available run time was not long enough for the shock width to saturate, although the effect of the finite system width is apparent as we see the $W = 256$ and $W = 1024$ curves separate for $t > 400$. We expect that for W large enough there will an "asymptotic" time regime for the growth of $\sigma(t)$ before it saturates, with behavior given by equations (6–8).

The results in Figure 2 indicate that the growth of fluctuations has not reached the asymptotic (in time) regime. If we think of the exponent β characterizing this growth as a time-dependent quantity, then $\beta \to .17$ for the longest times that we were able to observe (in the $W = 1024$ system), and is apparently still increasing. It may be that the long time behavior will still be consistent with the predictions of the linear KPZ equation given in (6–8), but that the approach to this asymptotic behavior is extremely slow.

There appear to be two reasons for this slow convergence. First, the shock width at $t = 0$ does not strictly vanish. There are fluctuations inherent to the initializing process of setting down particles randomly with probability ρ_0. This accounts for a "zero point fluctuation" of a few lattice spacings. We can eliminate this effect by starting with an artificially perfectly flat interface. The true asymptotic behavior will not be affected by this.

This, however, is not the main problem—the main difficulty is that there are natural, short wavelength fluctuations which result from the dynamics and form at an early time. Letting $\langle\cdot\rangle$ represent an average over the random dynamics, *i.e.* a sampling average, we see that there is a natural separation distance $\langle|(h(y,t) - h(y+1,t))|\rangle$ between the shock locations in neighboring rows, which builds up rapidly and then saturates. If the perpendicular jump rate is small, then this length can be quite large. In this case, $p_\perp \ll p_{\mathrm{left}} + p_{\mathrm{right}}$, neighboring rows are essentially noninteracting for long periods of time. The first particles in each row then execute a random walk relative to each other and can become quite distant. As their distance increases, it becomes more probable to have a transition from one row to another which will reduce the distance between the first particles in the two rows. These perpendicular transitions prevent the first particles in neighboring rows from moving arbitrarily far from each other (confinement), and thus $\langle |h(y,t) - h(y+1,t)| \rangle$ approaches an asymptotic value. For the jump rates we used, we found that this natural extension was on the order of a few lattice spacings, just enough to mask the overall shock broadening which was typically less than 8 lattice spacings.

This latter problem could not be eliminated with a simple adjustment of the initial conditions or jump rates. Therefore, we looked at other manifestations of shock broadening which in the asymptotic time regime should be equivalent to the shock width defined above. Defining

$$G(m,t) = \langle h(y,t)h(y+m,t) \rangle - \langle h(y,t) \rangle^2, \tag{12}$$

we see that $G(0,t) = \sigma^2(t)$. For $m = 1$ or 2, $G(m,t)$ represents the nearest (row) neighbor, $m = 1$, and next nearest neighbor, $m = 2$, truncated first particle correlation functions. These functions have none of the $t = 0$ fluctuations mentioned above and will be affected to a much lesser extent by the short-wavelength fluctuations. In fact, $G(1)$ differs from $G(0)$ by exactly the nearest-neighbor fluctuations:

$$G(0,t) - G(1,t) = \frac{1}{2} \left\langle (h(y,t) - h(y+1,t))^2 \right\rangle. \tag{13}$$

In Figure 3 we show these functions and include the width ($m = 0$) for comparison. Note that for $m = 1$ and $m = 2$ that the "effective growth exponent," characterized by the slope of the tangent to this curve, is actually greater than .25 and is decreasing. For the width $m = 0$ it is increasing.

As well as studying $G(m,t)$ for fixed m and varying t, we considered the complementary case of fixed t and varying m. The results appear in Figure 4. The self-correlation ($m = 0$) is the square of the shock width.

As $G(m,t)$ decays exponentially in m (for m not too large), we can define a correlation length along the shock, $\xi_{||}(t)$, determined by

$$G(m,t) \sim \exp[-m\xi_{||}(t)] \tag{14}$$

for small m. In Figure 5 we show time time evolution of the correlation length. The asymptotic behavior corresponds to a diffusive growth: $\xi_{||} \sim t^{1/2}$; this is in agreement with the evolution determined by equation (4). Note that the initial behavior is much more rapid as the short wavelength fluctuations develop.

3.2.1 Linearized surface equation

The short wavelength fluctuations in the ASEP are of the same order of magnitude as the shock width and therefore mask its growth. We checked to see if this behavior persisted in a

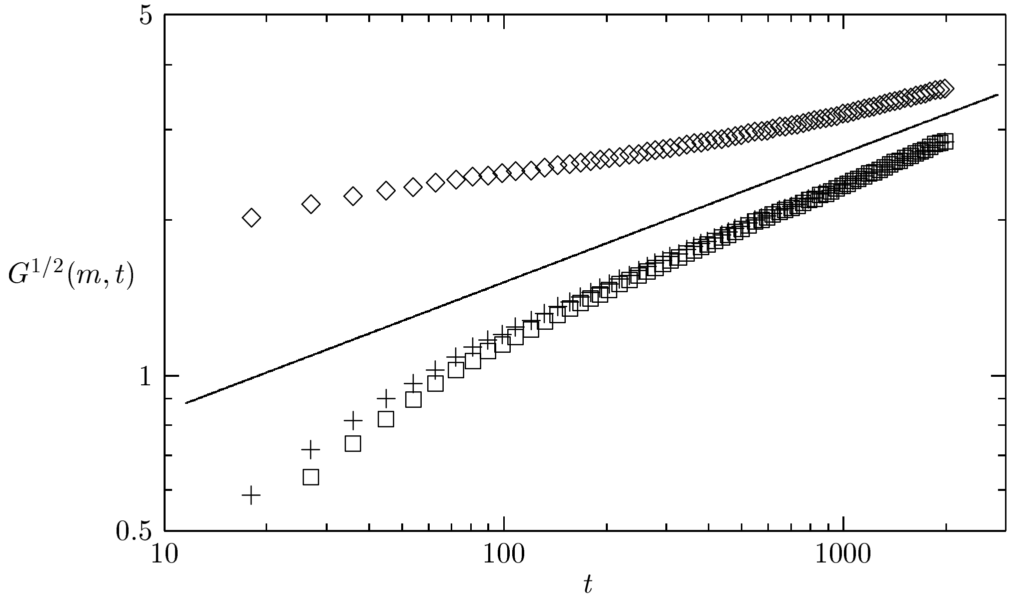

Figure 3: Time dependence of $G(m,t)$ for $W = 1024$. $m = 0(\diamond)$, $m = 1(+)$, $m = 2(\Box)$. Line has slope 1/4.

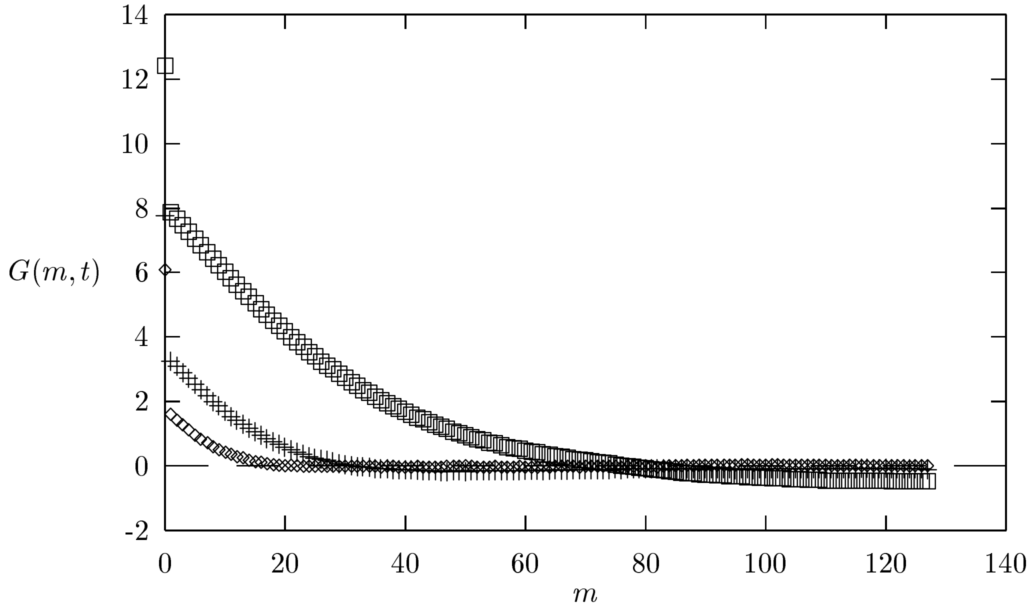

Figure 4: Correlations along the shock at times 36 ($\diamond$), 133(+), and 662($\Box$).

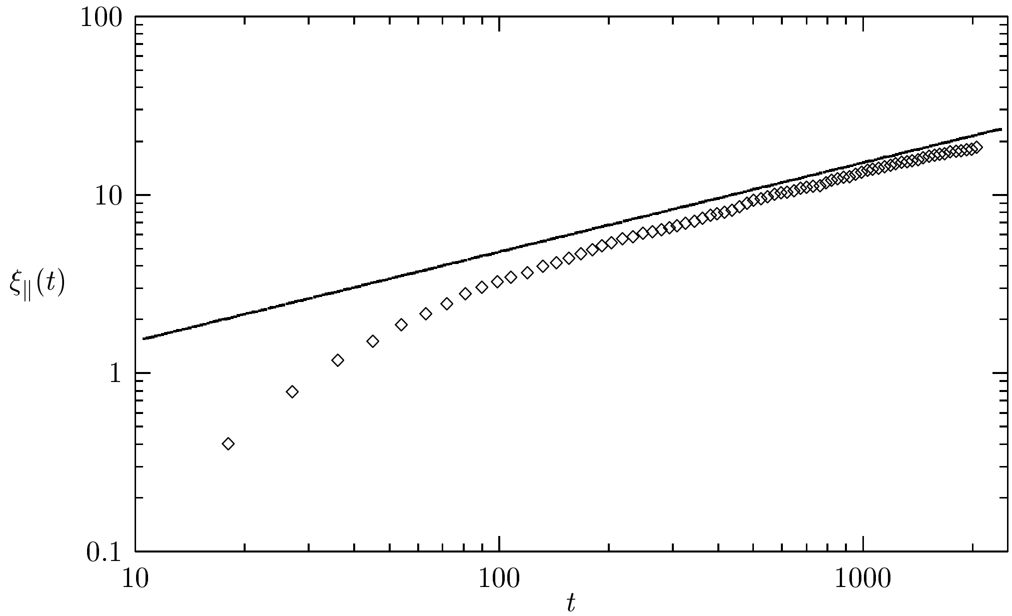

Figure 5: Growth of correlation length. $W = 1024$. Line has slope 1/2.

discretized version of the linear (1d) KPZ equation, where we know the asymptotics exactly. Consider the discretization of (4):

$$h(y, t+1) - h(y, t) = D[h(y-1, t) - 2h(y, t) + h(y+1, t)] + \gamma\zeta(y, t). \tag{15}$$

The noise term ζ is Gaussian with covariance

$$\langle \zeta(y, t)\zeta(y', t') \rangle = \delta(y - y')\delta(t - t'). \tag{16}$$

We solved for time dependence of the shock width and $m = 1$ correlations by simulating the process governed by (15) and (16). The size of the system (corresponding to the length of the interface which is the dimension of the ASEP perpendicular to the field, *i.e.* W) was 10000 sites, and we averaged over 50 independent samples. The diffusion constant is $D = 0.5$, and the noise amplitude is $\gamma = 0.5$. These parameters were chosen to compare with the results of the ASEP simulations. The initial conditions on $h(y, t)$ were equivalent to what would result from the initialization process outlined above with a density $\rho_0 = 0.5$.

What we found was qualitatively very similar to the simulations of the ASEP, and is presented in Figure 6. Namely, we observed an initial regime of fast growth in the nearest neighbor correlation function $G(1, t)$ and an eventual tapering off of the effective time-dependent exponent. Meanwhile, for $G(0, t)$ (shock width squared) we found that the effective growth rate *increased* with time consistent with an exponent $\beta = 1/4$.

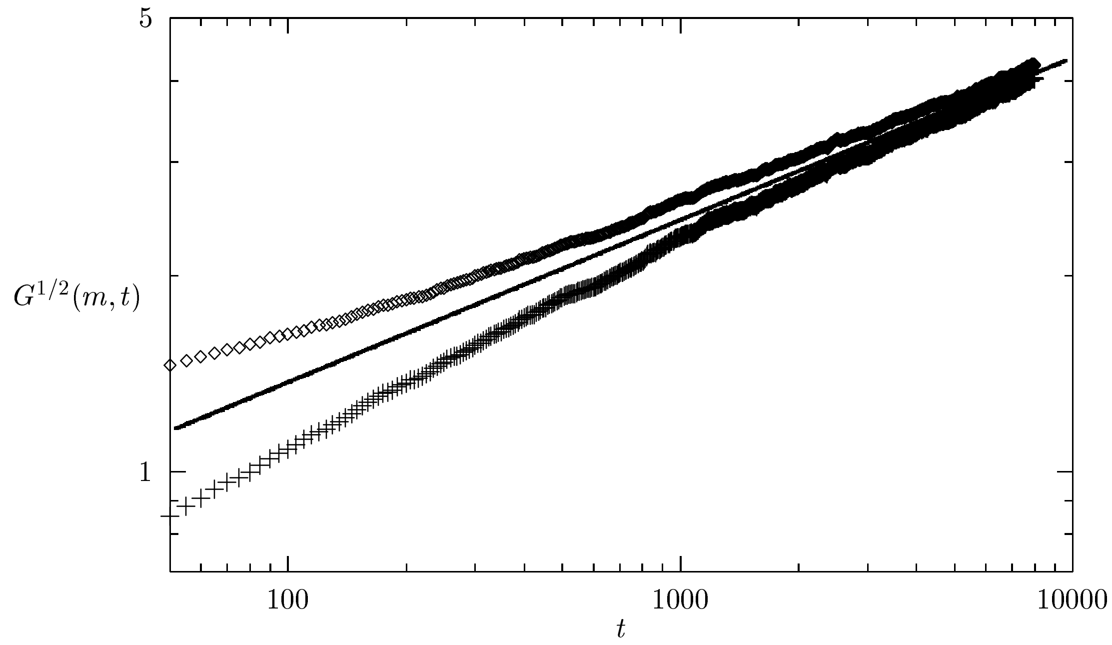

Figure 6: $G(m,t)$ for a discretized linear KPZ equation, $m = 0(\diamond)$ and $m = 1(+)$. Solid line has slope 1/4.

3.2.2 Compatibility with Existing Theory

We have presented computer simulations of the two dimensional asymmetric simple exclusion model. The growth of shock width in the ASEP is consistent with the current theory, but the natural width inherent to the dynamics make it difficult strengthen this claim. Since similar behavior is also observed in simulations of the discretized interface equation, we are, however, supportive of the linear theory.

4 Stationary Results

When we study the stationary state of our periodic model with a blockage, we have an advantage over the time-dependent case in that we need not worry about initial conditions—only the total particle number is relevant. Thus we need not worry about the best way to produce a shock, *e.g.* whether we should use a checkerboard pattern or simple product measure. However, this lessens the freedom we have in determining the type of shock that results. Since a shock in the stationary state must have no net drift, the densities on either side must be symmetric with respect to density 1/2 (the shock velocity, which must be zero in the stationary state, is given by $v_{\text{shock}} = 1 - \rho_{\text{left}} - \rho_{\text{right}}$). Thus the simple technique of identifying the shock by the first particle in each row, valid for $\rho_{\text{left}} = 0$, will not be effective.

4.1 Shock identity

The difficulty of identifying the shock also appeared in the one-dimensional case [16], where a so-called second class particle [19] was used to track the shock. The second class particle is an extra particle added to the system, which is treated as a hole in exchanges with particles and as a particle in exchanges with holes; this does not change the dynamics of the original particles. When the second class particle is in a high density region (of ordinary particles), it is forced to the left by the particles jumping (to the right) and landing on it; when it is in a low density region it moves to the right.

In two dimensions one can also add second class particles to the system, but as they can diffuse from row to row we no longer have a single second class particle associated with the shock position in a given row. One possibility is to add a large number of second class particles to the system and determine their distribution, unfortunately a computationally intensive procedure.

The second class particle is actually a much more powerful tool than we need for determining the shock position, so we discard it in favor of something simpler. The motion of the second class particle is basically that of a biased random walk with a drift towards the shock position; instead of second class particles we introduce shadow particles whose dynamics is *exactly* that of a biased random walk with a drift towards the shock position. These shadow particles do not affect the motion of the ordinary particles but move in a "potential" determined by the ASEP configuration. Specifically, after each sweep of Monte-Carlo updates, each shadow particle (of which there is one per row) moves according to the following rule:

$$h(y,t+1) = \begin{cases} h(y,t) & \text{with probability } 1/4, \\ h(y,t) - s(h(y,t),y;t) & \text{with probability } 3/4, \end{cases} \tag{17}$$

where $s(x,y;t) = 1$ if there is a particle at site (x,y) at time t, and $s(x,y;t) = -1$ if there is no particle there. Thus the shadow particles move to the left in regions of high density and to the right in regions of low density, driving them towards the shock where these regions meet. The probabilities $1/4$ and $3/4$ were chosen simply for convenience; other similar rules for the shadow particle evolution were tried but did not yield significantly different behavior.

Note that we continue to label the location of the surface by $h(y,t)$, even though our definition of this location has changed from the time-dependent case, where we made use of the first particle position, since both definitions represent the same physical idea. Ideally, one would like to allow the "shadow" random walk to evolve for a long time for each given ASEP configuration; under such conditions it is clear that the shadow particles will accurately identify the shock position, provided a shock does in fact exist. The ratio of one shadow update per ASEP Monte Carlo step is a compromise between the need to accurately identify the shock postion and the desire to reduce the computational load of tracking it.

Quantities studied

We were interested in studying both the shock profile as well as its fluctuations. To this end we computed the following quantities from the sampled shock positions $h(y,t)$, where $\langle\cdot\rangle$ represents a sampling (*i.e.* time) average:

- the average shock position $\langle \bar{h} \rangle = \left\langle \frac{1}{W} \sum_{y=1}^{W} h(y,t) \right\rangle = \frac{1}{W} \sum_{y=1}^{W} \langle h(y,t) \rangle$,

- the variance in the shock position $\langle \delta^2 \rangle = \left\langle (\bar{h}(t) - \langle \bar{h} \rangle)^2 \right\rangle$,

- the average shock width $\langle \sigma \rangle = \left\langle \left(\frac{1}{W} \sum_{y=1}^{W} (h(y,t) - \bar{h}(t))^2 \right)^{1/2} \right\rangle$,

- the rms shock width $\langle \sigma^2 \rangle^{1/2} = \left\langle \left(\frac{1}{W} \sum_{y=1}^{W} (h(y,t) - \bar{h}(t))^2 \right) \right\rangle^{1/2}$,

- the truncated height-height correlation function $\langle G(m) \rangle = \left\langle h(0,t)h(m,t) - \bar{h}^2(t) \right\rangle = \left\langle \frac{1}{W} \sum_{y=1}^{W} \left(h(y,t)h(y+m,t) - \bar{h}^2(t) \right) \right\rangle$.

4.2 Results

We attempted to determine the behavior of the shock width as we varied the size of our system. We found that if either the system size L or the system width W was taken very large, the shock width approached an asymptotic value. Thus we were able to reduce our two parameter system to a single parameter, by considering the regimes $L \gg W$ and $L \ll W$.

For $L \gg W$, the finite width of the system prevents the shock from growing indefinitely. This behavior should correspond to growth saturation in the time-dependent case. We present our data for a system with $\rho_{\rm avg} = 0.5$, $p_{\rm right} = 0.75$, $p_\perp = .125$ and $r = 0.25$ in Figure 7. The error bars (three symbols are plotted for each measurement: the actual value and that value shifted up or down by the error bound) represent statistical error based on the approximate number of independent samples selected from the steady state in each system. To fully saturate the shock width required that we consider a system length of 3200 for a system width of 180; typically we had $L > 16W$.

We only plot the data for the rms shock width; the average shock width behaved similarly. Along with $\langle \sigma^2 \rangle^{1/2}$ we plot the nearest neighbor correlation $\langle G(1) \rangle^{1/2}$ which should have the same asymptotic behavior as the shock width. The difference between the two is due to the short-wavelength fluctuations, just as in the time-dependent case. It is clear that we are just beginning to access the asymptotic behavior; our results are consistent with $\alpha = 0.5$ but cannot be considered conclusive.

For $L \ll W$, the finite width of the system is irrelevant to the width of the shock. In this case the system length L determines the shock width. We present our data for a system with $\rho_{\rm avg} = 0.5$, $p_{\rm right} = 0.75$, $p_\perp = .125$ and $r = 0.125$ in Figure 8. To reach the asymptotic shock width for the longest system, $L = 360$, required a system width of 720; typically we had $W > 2L$.

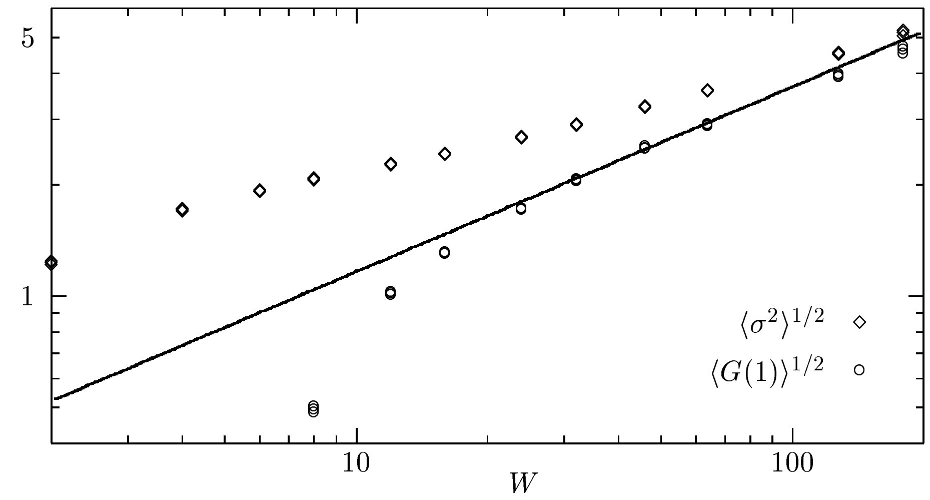

Figure 7: Shock width *vs.* system width W for $L \gg W$. Solid line has slope 0.5.

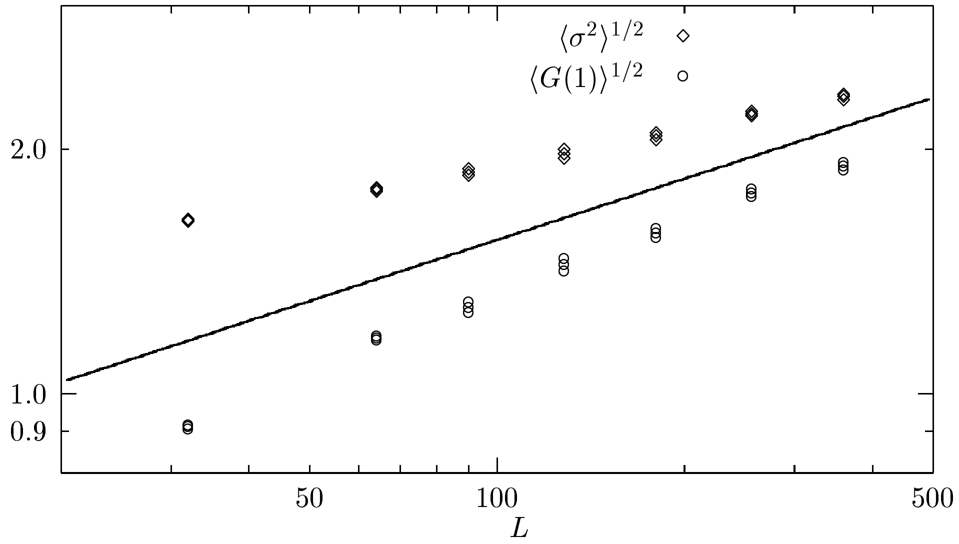

Figure 8: Shock width *vs.* system length L for $L \ll W$. Solid line has slope 0.25.

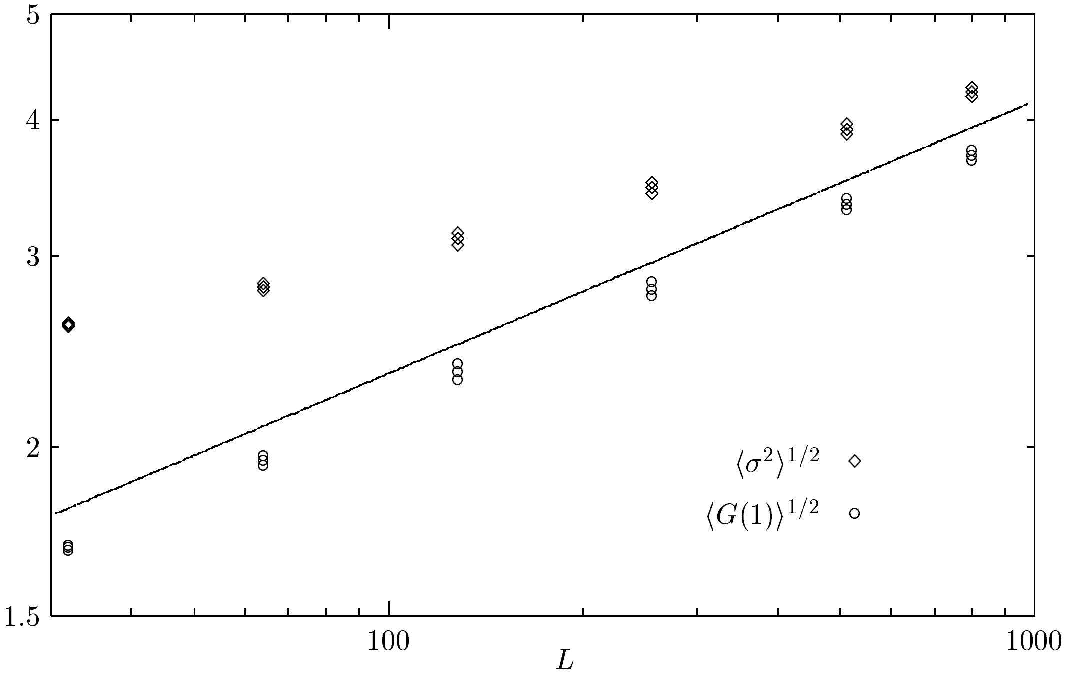

Figure 9: Shock width *vs.* system length L for the semi-parallel update model. Solid line has slope 0.25.

If one associates length with time, we should expect to see the same exponent β as we saw in the time-dependent case, *i.e.*

$$\langle\sigma^2\rangle^{1/2} \sim L^\beta \sim t^\beta \sim \sigma(t). \tag{18}$$

Indeed, our results are consistent with $\beta = 0.25$.

In an attempt to examine systems larger than 720×360, we used the random-sublattice updating technique described earlier. With a system width of 12870 we were able to examine lengths up to 800 and be quite sure that the finite width of the system was not affecting the shock width. We present the data from our semi-parallel model in Figure 9. The parameters are the same as for Figure 8, and the data is in fact very similar.

We should be somewhat careful in interpreting the results from our semi-parallel model, because there are differences from the serial model. In Figure 10 we plot the height-height correlation function G for the ASEP with length $L = 64$ and width $W = 256$, along with the semi-parallel model with the same length. Although both systems have an initial exponential decay, the serial model has a significantly larger "dip" of negatively correlated surface heights than that which we see in the semi-parallel model.

The basic structure of the shock seems to be fairly impervious to the details of the model. The scaling behavior of its intrinsic width, for example, does not depend upon the overall density ρ_{avg}. On the other hand, the location $\bar{h}$ and the fluctuations of that location *do* depend upon ρ_{avg}, specifically, whether or not $\rho_{\text{avg}} = 0.5$. This is the same behavior observed in the

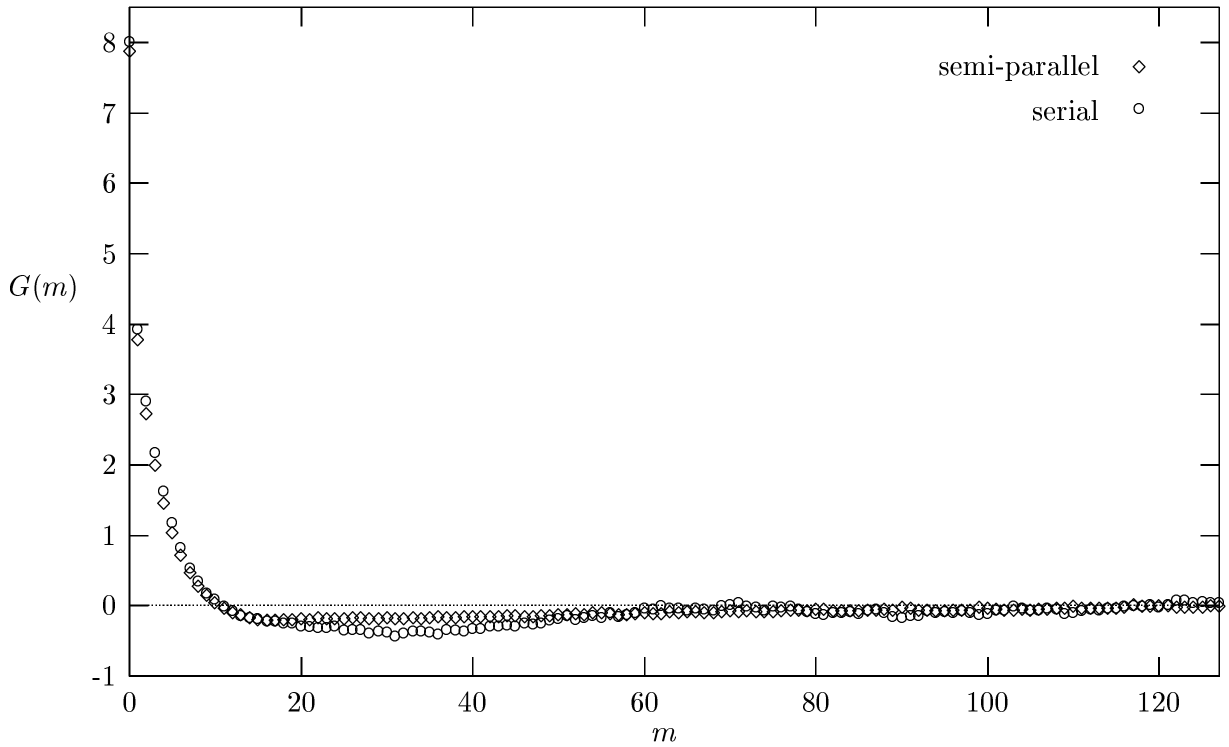

Figure 10: Height-height correlation function.

one-dimensional model, where the shock fluctuations were reduced when there was particle-hole symmetry [16].

For a system where $L \gg W$, we would expect the system to be effectively one-dimensional, and we recover the one-dimensional results [16]. For $\rho_{\rm avg} \neq 0.5$, we expect $\left\langle(\bar{h}(t) - \langle\bar{h}\rangle)^2\right\rangle^{1/2}$ to scale like $L^{1/2}$. In Figure 11 we plot the shock fluctuation, rescaled by the square root of the system width, against the system length. The system parameters are $\rho_{\rm avg} = 0.5625$, $p_{\rm right} = 0.75$, $p_\perp = .125$ and $r = 0.25$. It is clear from this data that

$$\langle\delta^2\rangle = \left\langle(\bar{h}(t) - \langle\bar{h}\rangle)^2\right\rangle \sim \frac{L}{W}. \tag{19}$$

The collapse of the data shows that this scaling is valid even for quite narrow systems ($W = 4$). Thus the $\rho_{\rm avg} \neq 0.5$, two-dimensional system behaves as a collection of W independent one-dimensional systems, at least as far as the overall fluctuations of the shock position is concerned.

The situation is different when $\rho_{\rm avg} = 0.5$. The only difference between the data in Figure 12 and Figure 11 is that in Figure 12 we have $\rho_{\rm avg} = 0.5$. Here the rescaled data for different system widths superimpose on each other only for L small (compared with W). Examining the data in Figure 12 carefully, we see that the fluctuations for each width cross over from $L^{1/4}$ behavior to $L^{1/3}$ behavior, with the crossover point increasing with W. The fact that the data superimposes for small L indicates that in this regime fluctuations scale as $L^{1/4}/W^{1/2}$, while the $L^{1/3}$ behavior scales with a power of W different from 1/2. To get a better handle on this phenomenon, we plot the rescaled fluctuations against the system width in Figure 13. For $L \gg W$ the slope

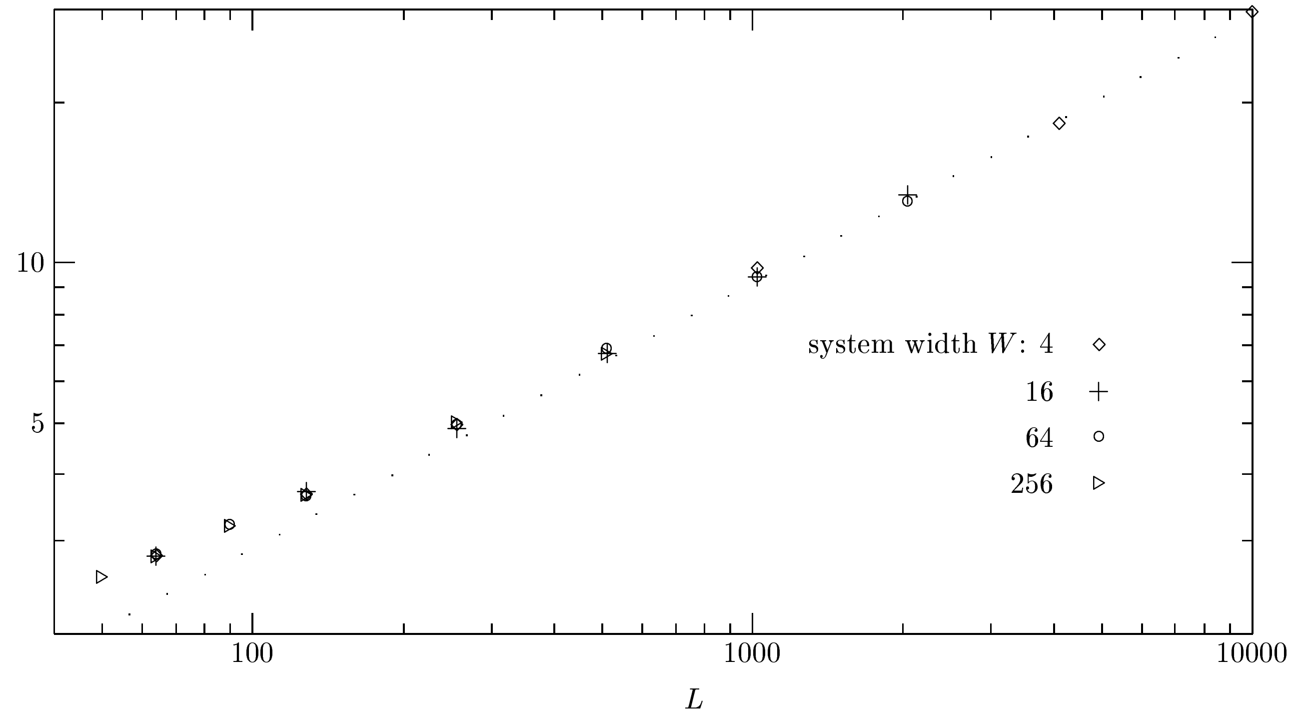

Figure 11: Rescaled shock fluctuation: $W^{1/2}\left\langle(\bar{h}(t)-\langle\bar{h}\rangle)^2\right\rangle^{1/2}$ *vs.* system length L. Average density different from 1/2. The dotted line has slope 1/2.

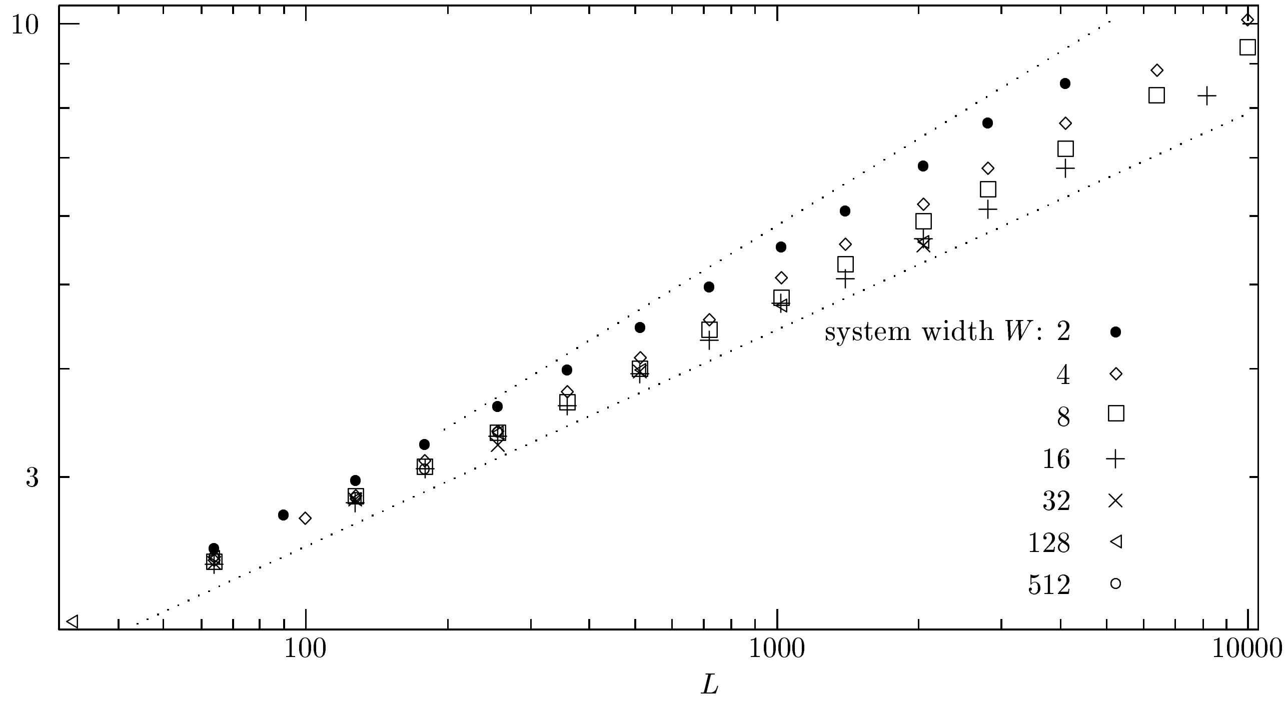

Figure 12: Rescaled shock fluctuation: $W^{1/2}\left\langle(\bar{h}(t)-\langle\bar{h}\rangle)^2\right\rangle^{1/2}$ *vs.* system length L. Average density is 1/2. Dotted lines have slope 1/4 and 1/3.

approaches $-1/6$, which indicates that the fluctuations scale as $L^{1/3}W^{-1/2-1/6} = L^{1/3}/W^{2/3}$. While we do not have a complete understanding of this exponent, its makes sense from general scaling arguments as the crossover from $L^{1/4}$ to $L^{1/3}$ occurs when

$$L^{1/4}/W^{1/2} \sim L^{1/3}/W^{2/3}, \tag{20}$$

or when $L \sim W^2$—*i.e.* we observe one-dimensional behavior when particles have a chance to diffuse across the entire width of the system.

We can also think of the system at $L \gg W$ as a pseudo-one-dimensional system where the noise is reduced from that in the one-dimensional ASEP because of the average over the width. If we insert a noise intensity parameter I into the (one-dimensional) KPZ equation (2), *i.e.* the fluctuating Burgers equation [8, 12], yielding

$$\frac{\partial h}{\partial t} = \nu\frac{\partial^2 h}{\partial x^2} + \frac{\lambda}{2}\left(\frac{\partial h}{\partial x}\right)^2 + I\zeta(x,t), \tag{21}$$

then effectively $I \propto W^{-1/2}$. A scaling analysis of Amar and Family [20] indicates that fluctuations in h are proportional to $I^{4/3}$, so that we obtain fluctuations proportional to $W^{-2/3}$. This factor multiplies $L^{1/3}$ which is the behavior of the fluctuations in the one-dimensional system [16, 21, 22, 23, 12]. This is confirmed by simulations we have performed on the one-dimensional ASEP [24]. For hole density ρ_h $(=1-\rho)$ we find that the fluctuations in the shock position scale as $\rho_h^{2/3}t^{1/3}$, which is consistent with [20] since $I \sim \rho_h^2$.

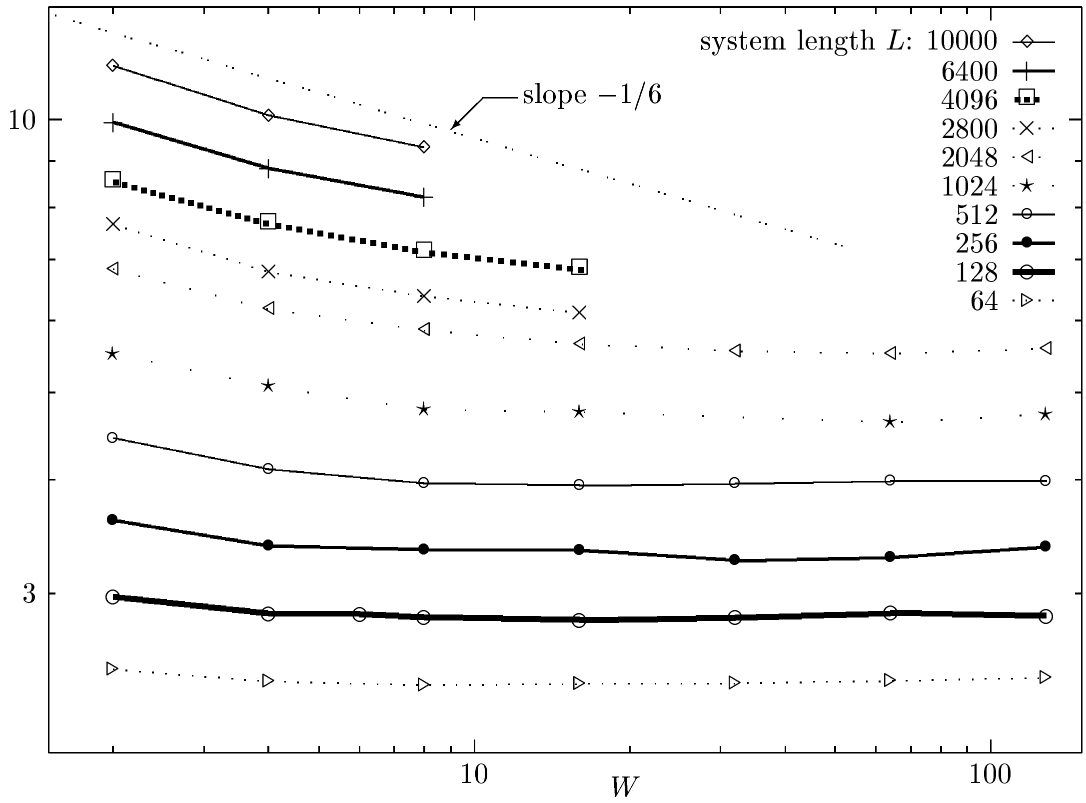

Figure 13: Rescaled shock fluctuation: $W^{1/2}\left\langle(\bar{h}(t)-\langle\bar{h}\rangle)^2\right\rangle^{1/2}$ *vs.* system width W. Average density is 1/2.

Table 1: Scaling behavior for the variance in shock position $\langle\delta^2\rangle$ and shock width $\langle\sigma^2\rangle^{1/2}$.

	$\rho_{\text{avg}} = 1/2$		$\rho_{\text{avg}} \neq 1/2$	
	$L \gg W$	$L \ll W$	$L \gg W$	$L \ll W$
$\langle\delta^2\rangle$	$(L/W^2)^{2/3}$	$(L/W^2)^{1/2}$	L/W	
$\langle\sigma^2\rangle^{1/2}$	$W^{1/2}$	$L^{1/4}$	$W^{1/2}$	$L^{1/4}$

This crossover point also makes sense from the point of view of understanding the $L^{1/4}/W^{1/2}$ behavior of the fluctuations in the shock position, and connects this with the $L^{1/4}$ behavior of the shock width. For $L \ll W^2$ treat each row of the system as an almost independent one-dimensional ASEP. By "almost" we mean we allow coupling only through the total density in each row; otherwise the rows are treated independently.

If a particular row has a density of ρ_{row}, its (local) shock position will have variance proportional to $|\rho_{\text{row}} - 1/2|L$ [16]. The diffusive coupling between rows will produce fluctuations in $\rho_{\text{row}} - 1/2$ that are $O(L^{-1/2})$. Thus the typical deviation of the local shock from the center of the system is $\left(O(L^{-1/2})L\right)^{1/2} = O(L^{1/4})$. This is the correct contribution to the shock width. The overall shock position is the average of the local shock position; we are treating each of the W local positions as an independent random variable, so the standard deviation of the average is $W^{-1/2}O(L^{1/4})$. Of course this neglects the $L^{1/3}$ term which must eventually be larger.

Our results for the stationary model are summarized in Table 1.

5 Discussion

5.1 Relationship Between Stationary and Time-Dependent Models

Studying the time-dependent behavior of the ASEP is significantly different from studying the stationary states of the ASEP with a blockage. While there is no rigorous argument that the same exponents should describe both the time-dependent and size-dependent scaling of the shock width, it is not suprising to expect that they are the same, considering that the underlying physics is identical in both models. Namely, the transit time for traversal of the distance from block to shock is of order L, so that if the time dependence is t^β, the length dependence should be L^β. The experimental correspondence is unmistakable—Figure 3, where we plot the correlations G *vs.* time t, and Figure 8, where we plot the correlations *vs.* system length L, are virtually copies of each other.

Of course, our only interpretations of this phenomenon are heuristic. Although it is clear that fluctuations due to the transit time will produce L^β behavior, we can not exclude the existence of stronger noise sources which would overwhelm this behavior—which in fact we do observe when particle-hole symmetry is broken.

5.2 Difficulties

The precise determination of scaling exponents, particularly small ones, is often not a straightforward task. This is especially true if one is limited in analyzing the range over which the scaling holds. In our case the constraints on simulation run-time, due to lattice size and computer memory considerations, proved crucial.

There were several options available to us which would have alleviated these problems, but all involved tampering with the ASEP dynamics, usually by destroying (or introducing spurious) correlations—small perturbations in models such as the ASEP that have a conservation law but do not satisfy detailed balance can have dramatic global effects [15]. It was precisely the ASEP, and not some approximate variant, that we wished to study. As a result, we were forced to simulate a truly two-dimensional problem and not just some restricted (effectively one dimensional) domain containing the shock surface.

5.3 Parallel *vs.* Serial Models

The future of large-scale scientific computing will rely on massively parallel computers and thus systems with parallel dynamics. As opposed to certain disciplines where the utilization of parallelism has been difficult, there are no inherent problems with the use of parallelism in physics—certainly "real world" dynamics are parallel. However, although they may not accurately represent the real universe, serial models are generally more amenable to analytical study [4].

We attempted to utilize parallel models that differed only very slightly from the original serial models. Even so, we observed behavior that was significantly different in certain respects. Thus the parallel dynamics must be checked carefully for consistency with the serial dynamics.

5.4 Other Models

5.4.1 Non-infinite temperature

The ASEP dynamics can be viewed as the infinite temperature limit of a driven diffusive system where the jump rates of the particles depend on the local environment. Models with temperature are clearly more realistic models than those without it, and the immediate question is whether or not the behavior we have observed is limited to the infinite temperature case.

In one dimension we have found no significant difference in the behavior between infinite and finite temperature models. The addition of temperature makes the determination of the dependence of the current on the density more difficult, but once this has been done, the shock fluctuations scale as predicted by the fluctuating Burgers equation (with the appropriate J *vs.* ρ behavior) [24].

In two dimensions many driven diffusive systems exhibit a phase transition [25, 26]; the low temperature behavior is qualitatively different from the ASEP. At higher temperatures, the behavior is at least qualitatively similar to the ASEP, in that shocks form and we can have segregation perpendicular to the field as in our stationary model [14], but we have no detailed data on the behavior of the interface.

5.4.2 Non-lattice models (*e.g.* molecular dynamics)

In addition to studying more realistic lattice models, it would be interesting to examine the behavior of models in continuous space. Specifically, we would like to study via nonequilibrium molecular dynamics simulations [27] the statistics of shocks that form when a compressible fluid is forced to flow through a pinched tube.

Acknowledgments

We thank Henk van Beijeren and Herbert Spohn for their contributions to this work. This work was conducted using the computational resources of the Pittsburgh Supercomputing Center.

References

[1] J. L. Lebowitz, E. Presutti and H. Spohn: "Microscopic Models of Hydrodynamic Behavior," *J. Stat. Phys.* **51**, 841–862 (1988).

[2] J. M. Burgers: "A mathematical model illustrating the theory of turbulence," *Adv. Appl. Mech.* **1**, 171 (1948).

[3] T. Tatsumi: "Theory of homogeneous turbulence," *Adv. Appl. Math.* **20**, 39–133 (1980).

[4] H. Spohn: *Large Scale Dynamics of Interacting Particles*, Berlin: Springer, 1991.

[5] A. De Masi, C. Kipnis, E. Presutti and E. Saada, "Microscopic structure at the shock in the asymmetric simple exclusion," *Stochastics and Stochastics Reports* **27**, 151–165 (1989).

[6] J. Krug and H. Spohn: in *Solids Far From Equilibrium: Growth, Morphology and Defects*, C. Godrèche, ed., Cambridge University Press, 1990.

[7] M. Kardar, G. Parisi and Y.-C. Zhang: *Phys. Rev. Lett.* **56**: 889 (1986).

[8] E. Medina, T. Hwa, M. Kardar and Y. C. Zhang: *Phys. Rev. A* **39**: 3053 (1989).

[9] K. Ravishankar: "Interface fluctuations in the two dimensional weakly asymmetric simple exclusion," *Stochastic Processes and Their Applications*, to appear.

[10] F. Family: "Dynamic Scaling and Phase Transitions in Interface Growth," *Physica A* **168**, 561–580 (1990).

[11] H. van Beijeren, R. Kutner and H. Spohn: "Excess Noise fpr Driven Diffusive Systems," *Phys. Rev. Lett.* **54**, 2026–2029 (1985).

[12] H. van Beijeren: "Fluctuations in the Motions of Mass and of Patterns in One-Dimensional Driven Diffusive Systems," *J. Stat. Phys.* **63**, 47–58 (1991).

[13] H. van Beijeren: private communication.

[14] J. V. Anderson and K.-t. Leung: "Effects of translational symmetry breaking induced by the boundaries in a driven diffusive system," *Phys. Rev. B* **43**, 8744–8746 (1991).

[15] P. L. Garrido, J. L. Lebowitz, C. Maes and H. Spohn: "Long-range correlations for conservative dynamics," *Phys. Rev. A* **42**, 1954–1968 (1990).

[16] S. A. Janowsky and J. L. Lebowitz, "Finite Size Effects and Shock Fluctuations in the Asymmetric Simple Exclusion Process," *Phys. Rev. A* **45**, 618–625 (1992).

[17] P. Ferrari: "The simple exclusion process as seen from a tagged particle," *Ann. Prob.* **14**, 1277–1290 (1986).

[18] D. W. Wick: "A dynamical phase transition in an infinite particle system," *J. Stat. Phys.* **38**, 1015–1025 (1985).

[19] C. Boldrighini, C. Cosimi, A. Frigio and M. Grasso-Nuñes: "Computer simulations of shock waves in completely asymmetric simple exclusion process," *J. Stat. Phys.* **55**, 611–623 (1989).

[20] J. G. Amar and F. Family: "Universal Scaling Function and Amplitude Ratios in Surface Growth," preprint (1991).

[21] J. Gärtner and E. Presutti: "Shock fluctuations in a particle system," *Ann. Inst. Henri Poincaré*, Section A: **53**, 1–14 (1990).

[22] P. Dittrich: "Travelling waves and long-time behaviour of the weakly asymmetric exclusion process," *Prob. Theory and Related Fields* **86**, 443–455 (1990).

[23] Z. Cheng, J. L. Lebowitz and E. R. Speer: "Microscopic shock structure in model particle systems: the Boghosian Levermore cellular automaton revisited," *Comm. Pure Appl. Math.* **XLIV**, 971–979 (1991).

[24] F. J. Alexander, S. A. Janowsky, J. L. Lebowitz and H. van Beijeren, in preparation.

[25] S. Katz, J. Lebowitz and H. Spohn: "Nonequilibrium Steady States of Stochastic Lattice Gas Models of Fast Ionic Conductors," *J. Stat. Phys.* **34**, 497–537 (1984).

[26] P. L. Garrido, J. Marro and R. Dickman: "Nonequilibrium Steady States and Phase Transitions in Driven Diffusive Systems," *Ann. Phys.* **199**, 366–411 (1990).

[27] D. J. Evans and G. P. Morriss: *Statistical Mechanics of Nonequilibrium Liquids*, San Diego: Academic Press, 1990.